ANL/ESD/12-15

Geothermal life cycle assessment – Part 3

Energy Systems Division

About Argonne National Laboratory

Argonne is a U.S. Department of Energy laboratory managed by UChicago Argonne, LLC under contract DE-AC02-06CH11357. The Laboratory's main facility is outside Chicago, at 9700 South Cass Avenue, Argonne, Illinois 60439. For information about Argonne and its pioneering science and technology programs, see www.anl.gov.

Availability of This Report

This report is available, at no cost, at http://www.osti.gov/bridge. It is also available on paper to the U.S. Department of Energy and its contractors, for a processing fee, from:

U.S. Department of Energy
Office of Scientific and Technical Information
P.O. Box 62
Oak Ridge, TN 37831-0062
phone (865) 576-8401
fax (865) 576-5728
reports@adonis.osti.gov

Disclaimer

This report was prepared as an account of work sponsored by an agency of the United States Government. Neither the United States Government nor any agency thereof, nor UChicago Argonne, LLC, nor any of their employees or officers, makes any warranty, express or implied, or assumes any legal liability or responsibility for the accuracy, completeness, or usefulness of any information, apparatus, product, or process disclosed, or represents that its use would not infringe privately owned rights. Reference herein to any specific commercial product, process, or service by trade name, trademark, manufacturer, or otherwise, does not necessarily constitute or imply its endorsement, recommendation, or favoring by the United States Government or any agency thereof. The views and opinions of document authors expressed herein do not necessarily state or reflect those of the United States Government or any agency thereof, Argonne National Laboratory, or UChicago Argonne, LLC.

ANL/ESD/12-15

Geothermal life cycle assessment – Part 3

prepared by
J. L. Sullivan, E. D. Frank, J. Han, A. Elgowainy, M. Q. Wang
Energy Systems Division, Argonne National Laboratory

November 2012

Geothermal Life Cycle Assessment – Part 3

J. L. Sullivan, E. Frank, J. Han, A, Elgowainy, and M. Q. Wang

Abstract

A set of key issues pertaining to the environmental performance of geothermal electric power have been addressed. They include: 1) greenhouse gas emissions (GHG) from geothermal facilities, 2) the use of supercritical carbon dioxide ($scCO_2$) as a geofluid for enhanced geothermal systems (EGS), 3) quantifying the impact of well field exploration on the life cycle of geothermal power, and finally 4) criteria pollutant emissions for geothermal and other electric power generation. A GHG emission rate (g/kWh) distribution as function of cumulative running capacity for California has been developed based on California and U. S. government data. The distribution is similar to a global distribution for compared geothermal technologies. A model has been developed to estimate life cycle energy of and CO_2 emissions from a coupled pair of coal and EGS plants, the latter of which is powered by $scCO_2$ captured from coal plant side. Depending on the CO_2 capture rate on the coal side and the CO_2 consumption rate on the EGS side, significant reductions in GHG emissions were computed when the combined system is compared to its conventional coal counterpart. In effect, EGS CO_2 consumption acts as a sequestration mechanism for the coal plant. The effects CO_2 emissions from the coupled system, prompt on the coal side and reservoir leakage on the EGS side, were considered as well as the subsequent decline of these emissions after entering the atmosphere over a time frame of 100 years. A model was also developed to provide better estimates of the impact of well field exploration on the life cycle performance of geothermal power production. The new estimates increase the overall life cycle metrics for the geothermal systems over those previously estimated. Finally, the GREET model has been updated to include the most recent criteria pollutant emissions for a range of renewable (including geothermal) and other power generating technologies.

1. INTRODUCTION

Reliable and affordable electric power provides invaluable support for the U.S. standard of living, and its ready availability is a key enabler of the U.S. industrial and commercial sectors. About 40% of our primary energy consumption is devoted to generating electric power and most of it is derived from fossil resources [EIA, 2010]. However, concern over climate change and energy security has prompted a reevaluation of U.S. primary energy consumption, especially from fossil resources. In efforts to reduce fossil fuel consumption, some states have already adopted "Renewable Portfolio Standards" and hence, are adding more wind, solar, and others to their sets of generating technologies. The EIA [2010] projects that renewable electricity, which now represents around 8.5% of U.S. electricity generation, will increase to about 17% by 2035. Most of this increase is projected to come from additional wind turbines and biomass combustion plants. However, geothermal electricity generation is another renewable generating technology that can significantly enable reductions in fossil fuel consumption. It is also expected to grow, especially considering the development of enhanced geothermal systems (EGS), which can effectively operate on the more broadly available, lower-temperature geofluids.

This report is the fifth in a series of LCA reports [Sullivan et al, 2010 & 2011 and Clark et al, 2010, 2011] on geothermal power and its comparison to other power production technologies. The other technologies included coal boiler and integrated gasification combined cycle (IGCC), natural gas combined cycle (NGCC), pressurized and boiling water nuclear reactors (N-PWR and N-BWR) for conventional thermoelectric facilities and representing renewable technologies were hydroelectric, photovoltaic (PV), wind, biomass combustion boiler and IGCC, and concentrated solar power (CSP). Also included in the renewable were the geothermal technologies including hydrothermal flash (HT-F), hydrothermal binary (HT-B), enhanced geothermal systems (EGS), and two variants of geo-pressured gas and electric from reworked (GPGE-rw) and green field sites (GPGE-gf). GPGE and CSP plants are termed hybrid facilities. The former co-produces fossil (gas) and renewable energy (geothermal electricity) and the latter either coproduces solar and gas power (assumed here to be a combined cycle turbine) or use natural gas for auxiliary purposes during operation. The LCA in this report covers both fuel cycle and materials and energy for power plant construction (plant cycle). From the earlier reports, key conclusions per kWh of electricity delivered include: 1) fossil plants have by far the greatest life cycle greenhouse gas emissions (GHGs) of all the technologies, 2) of the renewable technologies, biomass combustion, HT-F, and GPGE have the highest GHGs, 3) conventional thermoelectric plants (coal, natural gas, nuclear, and biomass combustion) require the least materials, 4) renewable power technologies require more materials, especially hydroelectric, EGS, 5) of all materials cement/concrete and steel are used to greatest extent across all generation technologies except for PV, and 6) GHG emissions from the plant cycle are greatest

for the renewable power technologies, with PV and EGS having the most. Most of these results have already been incorporated into Argonne's "Greenhouse Gases, Regulated Emissions and Energy in Transportation – GREET" model [GREET1, 2012; Wang, et al, 1999].

Despite the work already completed on the life cycle performance of geothermal power, there remain tasks to be completed. For example, the life cycle performance of geothermal power is impacted by greenhouse gases emitted during power production, and by exploration activities during plant and well field development. The latter can potentially have a significant impact of well field development. Supercritical carbon dioxide ($scCO_2$) has been advanced as a substitute for brine geofluids used in EGS systems for purposes of greater energy extraction in some cases or when inadequate water resources are available for conventional EGS. The life cycle implications of this approach have not been elucidated. Another important set of life cycle metrics is to determine criteria pollutant emission rates (g/kWh) from geothermal and other power plants. GREET computes fossil, petroleum, and total energy use (including renewable energy in biomass), emissions of greenhouse gases (CO_2, CH_4, and N_2O), and emissions of six combustion pollutants: carbon monoxide (CO), volatile organic compounds (VOCs), nitrogen oxides (NO_x), sulfur oxides (SO_x), particulate matter with a diameter below 10 micrometers (PM_{10}), and particulate matter with a diameter below 2.5 micrometers ($PM_{2.5}$). GREET includes electrical power generation from fossil fuels, nuclear fuels, and from renewable energy sources including solar and geothermal power production with hydrothermal and water-EGS technologies.

The purpose of this report is to present our results and findings in the areas sited above. More specifically, status of our assessment of the distribution of GHG emissions from U.S. geothermal power plants is presented with recommendations for acquiring improved data. Also given are LCA modeling results of the use of scCO2 derived from fossil plants in EGS scenarios and its impact on carbon sequestration. In addition, a model has been developed to estimate the impact of well field exploration on the LCA of geothermal facilities. And finally, results are presented and contrasted on criteria pollutant emissions among various power generation technology including geothermal power and their subsequent integration into the GREET.

2. METHOD

The methodology used herein is the same as previously discussed [Sullivan et al , 2010, 2011]. The life-cycle calculations presented herein are based on process life-cycle assessments, often referred to as process chain analyses (PCAs). This approach strictly employs detailed process specific-data that (ideally) are fully speciated in terms of purchased energy units (e.g., liters [L], kilowatt-hours [kWh], cubic meters [m^3], kilograms [kg], tonnes), specific materials consumption levels (e.g., tons, kg, tonnes), and emissions (g, kg, other). If such values for energy are not available, megajoule (MJ) or British thermal unit (Btu) values are acceptable, although less desirable due to ambiguities on whether they represent high or low heat values and

on whether they are a life cycle or purchased energy values. All energy values employed herein are low heat values (LHV).

The system boundary for our study is depicted in Figure 1; the product is the lifetime of kWh of electricity at the wall outlet, unless stated otherwise. As the figure shows, the life-cycle stages covered are the fuel cycle and plant cycle stages. The former includes fuel production and fuel use during plant operation, and the latter consists of onsite plant construction activities and the production of materials comprising plant structures and equipment. Because plant decommissioning and recycling stages are expected to be only a fraction of plant cycle burdens which in turn are at most marginal in magnitude, they are not considered here.

For the plant cycle stage, the materials tracked were concrete, steel, aluminum, copper, glass, silicon, iron, and plastics which are needed for making plant buildings, wells, enclosures, and equipment (e.g., turbines, generators, heat exchangers, etc.). Also tracked for each scenario were plant performance characteristics, such as capacity, capacity factor, and lifetime. Determined material compositional data were normalized on a per-megawatt (MW) output capacity and are henceforth termed material-to-power ratios (MPRs). For solid materials, the units are tonnes (metric tons – mt) per MW of output capacity; in the case of liquids, the units are kiloliters – kl per MW. In the few cases where energy units were cited, the same term was used. The MPRs can be thought of as metrics based on a "hardware functional unit" (i.e., a MW of output capacity).

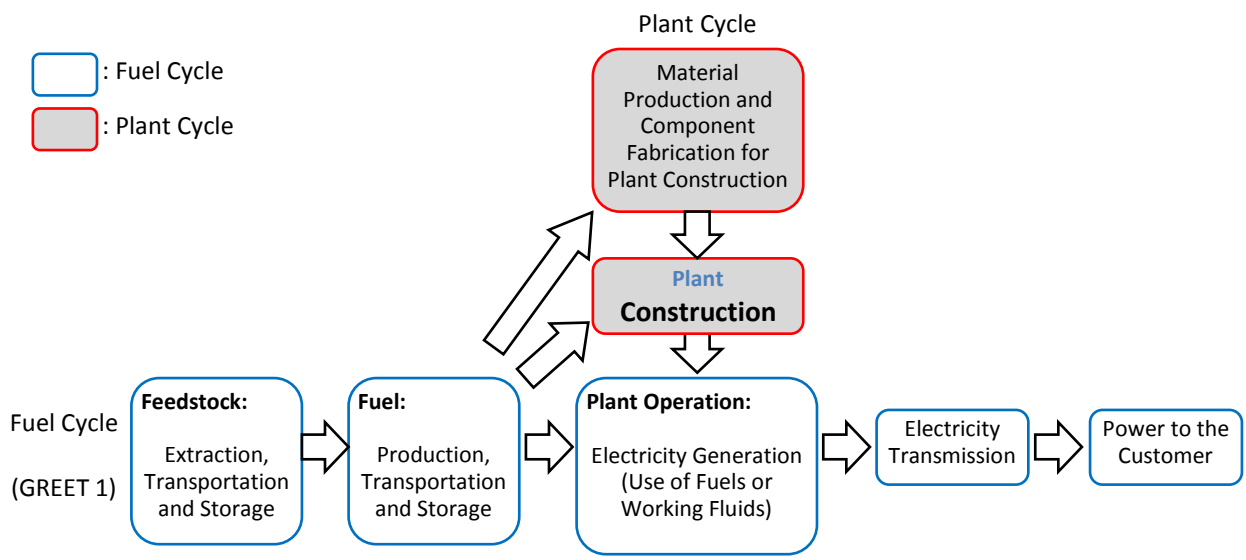

FIGURE 1: System Boundary for GREET Electricity Modules

MPRs were straightforwardly computed on the basis of facility material requirements divided by plant output capacity. In the case of EGS, HT-B and HT-F, capacity is based on a single output, i.e. MW_{el} of electric power. On the other hand, for GPGE there are two energy output flows, electric power (MW_{el}) and a natural gas production rate (MW_{th}). The sum of the

two is the facility output capacity, i.e. megawatt mixed (MW_{mx}). In cases where natural gas produced from GPGE facilities is burned on site to produce electricity, the output is solely electricity, i.e. MW_{el}.

Combining MPRs with plant capacity, lifetime, capacity factor, and fuel use and emissions incurred during the production of plant constituent materials yields two important service functional units for the plant cycle stage. They are the energy ratio ($\mathcal{E}_{pc} = E_{pc}/E_{out}$) and the CO_2-equivalent specific GHG emissions metric ($GHG_{pc} = \Sigma GHG_i/E_{out}$), where E_{pc} and E_{out} are the plant cycle energy use and total plant lifetime electricity delivered, respectively. The latter metric is a sum over a number of GHGs in terms of their CO_2-equivalent emissions (GHG_j). In addition to CO_2, the ones of most significance here are methane (CH_4) and nitrous oxide (N_2O). Values of $\mathcal{E}_{pc}$ and GHG_{pc} were estimated for the geothermal technologies and subsequently compared to other renewable and fossil technologies. After that, we compare overall fossil energy consumption and GHG emissions among the technologies, i.e. $\mathcal{E}_{tot}$ and GHG_{tot}, where the subscript "tot" denotes total across both plant and fuel cycles.

3. GHG Emission from U.S. Geothermal Facilities

During operation, there are GHG emitted from some geothermal facilities. Though in principle binary plants emit zero GHGs, finite and sometimes significant GHGs are released from flash plants, which currently represent the largest fraction of geothermal plant population in the U. S. For flash and dry steam plants, the geofluid gets exposed to the atmosphere during operation resulting in carbon dioxide and other gas releases. Bloomfield et al. [2003] reported a weighted average emission rate of 91 g/kWh of CO_2 from U.S. geothermal power plants. When considering the other GHG emission cited by them for these plants, namely methane, the total GHG emission rate becomes 110 g/kWh. Unfortunately, no mention of the range of U.S. geothermal emissions rates was given there [Bloomfield, 2003]. Their results were based on a study wherein, by agreement with geothermal plant operators, individual sources and values for provided emission rates remain confidential.

Since the geofluid in binary plants normally never gets exposed to the atmosphere, there are nominally no GHG emissions from them. This discussion solely pertains to non-binary plants, i.e. flash and steam plants. Because of this, the Bloomfield et al [2003] value needs further adjustment. Their capacity weighted average included the zero emissions from binary plants, which represented about 14% of the capacity surveyed at that time. When adjusted for flash plants only, their average GHG emission rate becomes 131 g/kWh (106 g/kWh for CO_2 only).

A comprehensive global survey of CO_2 emissions from global operation of geothermal power plants was conducted by Bertani & Thain [2001]. Other GHGs were not included. Their

generation emission rate data ranged from 4 to 740 g/kWh, obtained from 85 plants, representing 85% of global capacity, apparently for non-binary plants only. In fact, the weighted average for the global distribution is 122 g/kWh. While the global average is reasonably consistent to the adjusted weighted average from Bloomfield et al [2003], i.e. 106 g/kWh for CO_2 only, we are unable to draw any conclusions about the distribution of GHGs from U. S. non-binary geothermal facilities. From a GHG emission point of view, it is important to determine the U.S. geothermal GHG emission distribution. For example, the maximum global value just cited is about 40% more than the 528 g/kWh fuel cycle emissions [converted from wall outlet value in GREET1_2012 to the plant gate value using 6.5% transmission loss] for a NGCC plant operating at 49% efficiency.

The only publicly available information on GHG distributions from U.S. geothermal plants is provided by the California Environmental Protection Agency's Air Resources Board (CARB) [39]. Other states with geothermal facilities neither require nor routinely collect GHG emissions from such plants within their jurisdictions. Using the CARB GHG emissions data [CEPA, 2010] and electricity production data from those plants [EIA-923, 2010], we developed emission rates which were subsequently associated with the "running capacities" [GEA, 2012] of the corresponding plants. From a ranked list of emission rates vs. cumulative running capacity, an emission rate distribution curve was developed.

Figure 2 displays GHG emissions as a function of fraction of cumulative running capacity from geothermal plants both worldwide [Bertani and Thain, 2001] and those for California (CA). The global values shown in the figure are data from 85 plants aggregated into 50 g/kWh bins, ranging from 0 to 50 to over 500 g/kWh. The California geothermal emissions, on the other hand, arise from 13 individual values reported to CARB, some of which are aggregated values representing several plants and some representing single plants. The CA data correspond to values from 1,523 MW of running capacity for flash, double flash and steam plants, which is roughly a quarter of the global capacity (6,800 MW) surveyed by Bertani and Thain [2001]. The "CA" distribution shown in Figure 2 ranges from 11 to 370 g/kWh with a weighted average emission rate of 97.9 g/kWh. Though this value is not much lower than the adjusted Bloomfield et al [2003] average value, it does suggest that the CA non-binary distribution might be lower than the Bloomfield value, which covered more states than just California. On average, dry steam plants shown in Figure 2 look to have lower GHG emissions than flash plants, but this appearance might be due to a limited number of individual plant data.

The similarity of the global and CA non-binary emission distributions suggests that these trends might be representative of this class of geothermal technologies and associated resources. Based on the EIA data [EIA-923, 2010], California produces 83% of all U.S. geothermal electricity, and 93% of U.S. geothermal non-binary power (flash and steam). However, California geothermal GHG emissions are not representative of geothermal power production in other states. Only 6% of California's geothermal running capacity is derived from binary plants,

where as it is 63% for Nevada, 25% for Utah, and 100% for Hawaii and Idaho [GEA]. This is not surprising. California's geothermal power is derived from apparent hot geological resources whereas other states less endowed with such resources take advantage of lower temperature resources using binary technology.

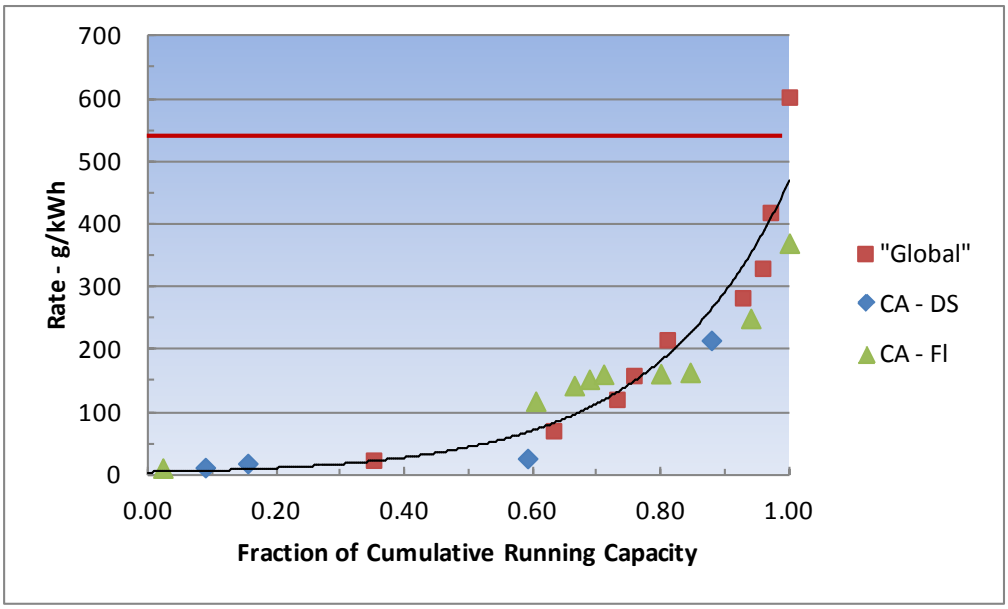

Figure 2: Operational CO_2 emissions per generated kWh from flash (Fl) and dry steam (DS) geothermal plants as a function of the fraction of considered plant running capacity for global and California production (CEPA, 2008); horizontal red line – fuel cycle emissions at the plant gate from a natural gas combined cycle plant [GREET1_2012].

Due to the use of actual electricity production values [EIA-923, 2010], the California emission rate distribution curve shown in Figure 2 is better than the previously [Sullivan et al, 2011] published curve where electricity production values were based on running capacity values [GEA]. Nonetheless, our estimate of this curve must be considered provisional, despite its similarity to the global curve. Firstly, there is no reason that the two distributions should agree. More significantly, there are limitations to existing California data which arise primarily from plant emission reporting requirements, including not all plants reporting, not all plants reporting all GHGs (CO_2 and CH_4), limited number of facility data points, and finally an unknown number of plants using a one size fits all emissions factor for its reported value instead of measured values. This emission factor, 7.53x10-3 g/btu heat extracted, corresponds to 25.7 g/kWh$_{heat}$, which when adjusted by an appropriate range of heat rates (5→ 6½ kWh$_{heat}$/kWh$_{elec.}$) varies from 129 to 162 g/kWh$_{elec}$. For this reason and the others just mentioned, the CA non-binary curve shown in Figure 2 might not truly represent the actual CA non-binary emission distribution.

Fortunately, starting in 2011 data submitted to CARB must be based on actual measured emission values. Once the data starts making its way through the CARB review process, more accurate assessments will become available for California GHG emissions from geothermal power plants.

Even with higher quality GHG data at hand, their significances can be called somewhat into question. The sites for most flash and steam geothermal power plants are locations where the resource is manifested at the surface. This includes hot springs, fumaroles, mud pots, steam vents and geysers. These features demonstrate the presence of hot resource and suggest that there is already a background level of GHGs naturally being released at those locations. The question at hand pertains to the degree which power plant activity impacts overall emissions (plant plus background) from the area. Further, will the GHG emissions decrease over time and if so by how much? Quantitative answers to these questions must await results from further research.

4. Supercritical CO2 as a working fluid

Existing geothermal electricity generation is almost entirely from geothermal resources where water and steam present in hot permeable rock are brought to the surface for power generation, but relatively few geothermal sites have hot rock perfused with water. Enhanced geothermal systems (EGS) inject water from nearby sources into dry geological structures and recover hot water to drive turbines, coupled through a secondary fluid with a low boiling point. EGS expands the potential for geothermal power, but adequate water must be available to deploy it (Tester 2006).

Brown proposed using supercritical carbon dioxide ($scCO_2$) instead of water to recover heat for EGS (Brown 2000). Electricity production from fossil fuels, especially from coal, produces CO_2 that could be captured, compressed to $scCO_2$. If this $scCO_2$ were available near a geothermal resource, it might be utilized for power production; moreover, while water loss below ground is a problem, $scCO_2$ consumption below ground provides the benefit of geological carbon storage.

Supercritical CO_2 requires energy to produce and transport so, although $scCO_2$ -EGS is an appealing idea for increasing geothermal power production, there are questions about net energy consumption when all activities ranging from $scCO_2$ production and transportation through power delivery are considered. Our goal here was to examine the energy consumption and emissions incurred when coal fired electricity is used to produce top off $scCO_2$ needed to replace CO_2 lost from the reservoir and when that $scCO_2$ is subsequently transported by pipeline to a geothermal site and utilized for power production. The scope of the study includes greenhouse gas (GHG) emissions and energy consumption associated with producing 1 MWh of total electricity before transmission. Activities related to procuring and using fuels (fuel cycle) and activities related to plant construction (plant cycle) are included. The fuel cycle includes the

production and transportation of $scCO_2$. A separate discussion of our treatment can be found elsewhere [Frank et al, 2012].

4.1 System Description

There are advantages and challenges from using $scCO_2$ compared to using water for geothermal heat recovery. Supercritical CO_2 has gas-like properties when propagating through rock and has viscosity 40% that of water [Brown 2000]. For certain conditions, these properties enable $scCO_2$ to permeate rock more easily than water. Further, $scCO_2$ density decreases enough when heated below ground that the buoyancy of hot $scCO_2$ can produce a thermal siphon effect that reduces pumping requirements. The low heat capacity of $scCO_2$ relative to water (roughly 40%) potentially offsets these advantages, but the low viscosity and thermal siphon effect can result in higher circulation rates so that, when considered on the basis of required pumping energy, estimated net heat production for $scCO_2$ is comparable to that of water [Brown 2000].

The $scCO_2$ consumption (storage) rate affects the system concept. Some researchers estimate $scCO_2$ consumption from experience with water-EGS. This approach estimates $scCO_2$ consumption to be 5% of the $scCO_2$ flow rate [Pruess and Azaroual 2006, Pruess 2007]. In one scenario, each MW of $scCO_2$ -EGS power would require 3 MW of coal-fired power to supply adequate $scCO_2$ to meet the $scCO_2$ -EGS consumption rate [Pruess 2007]. If consumption rates were this high, the geothermal system would require an $scCO_2$ pipeline to meet the $scCO_2$ demand. In this scenario, the $scCO_2$ -EGS system serves as a sequestration mechanism for the (upstream) fossil-based power plant that, in addition, generates renewable electrical power as a by-product of the sequestration process.

A contrasting scenario estimates much lower $scCO_2$ consumption [Dunn 2010, Mobley 2011]. The scenario considered by these authors utilizes deep impermeable rock as the heat source. There are four mechanisms that can result in loss of $scCO_2$ from the reservoir: hydrodynamic trapping in pores of a porous rock capped by impermeable rock; solubility trapping in water or other liquids such as crude oil within porous rock; adsorption trapping on organic matter in coal seams and shale; and mineral trapping from reactions with silicates resulting in immobilized carbonates [Nelson et al 2005]. In the stimulated (fractured) impermeable rock model of Dunn and Mobley, only mineral trapping is possible resulting in low consumption rates [Dunn 2010]. In one of their scenarios, consumption was only 0.1% of flow. In such a scenario, the $scCO_2$ consumption can be met with a moderately sized on-site generator, no pipeline is required, and almost 75% of the total power output derives from geothermal energy [Mobley 2011].

4.2 System boundary, and functional unit

The system boundary, depicted in Figure 3, includes coal mining, coal transportation to the power plant, and all operations at the power plant. For the $scCO_2$ -EGS, the system boundary also includes CO_2 capture, compression to $scCO_2$, transportation to the $scCO_2$ -EGS site, and power production. The activities just described represent the "fuel cycle". Energy and emissions for constructing the power plant infrastructure belong to the "plant cycle" and are also included. The functional unit is one kWh of electricity from the combined system, coal and EGS power facilities. Data from the GREET model were employed for both fuel and plant cycles of our combined system.

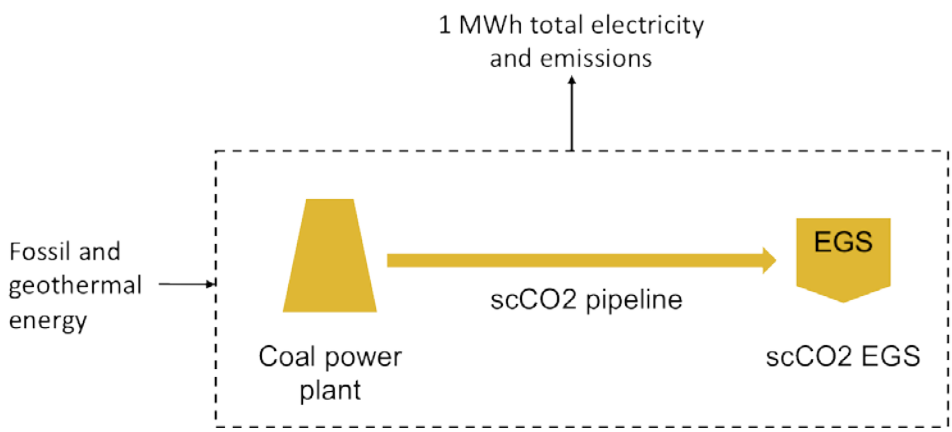

Figure 3: System diagram for $scCO_2$ **-EGS power.** A fossil power plant supplies the $scCO_2$ feedstock that is consumed (sequestered) during $scCO_2$ -EGS power generation.

The analysis presented in this work focused on the high-consumption scenario but examined a wide range of $scCO_2$ consumption rates. In the high-consumption scenario, an $scCO_2$ pipeline interconnects a fossil power plant and the $scCO_2$ geothermal power plant. The infrastructure materials for the $scCO_2$ pipeline interconnecting the fossil and $scCO_2$ plants and the energy consumption for its operation are also included.

4.3 Model

4.3.1 Reservoir development, size, and lifetime

Brown [2000] considers a reservoir in Precambrian crystalline rock developed by hydraulic fracturing with $scCO_2$. The pore fluid is dissolved in the $scCO_2$ and removed over a few weeks. We accounted for energy and emissions associated with plant material production, plant construction, well construction, well field stimulation, and plant to well piping (Sullivan et al 2010).

Turaga et al [2011] modeled thermal drawdown as a function of circulation given the thermal conductivity, density, specific heat capacity, and thermal diffusivity of rock, water, and $scCO_2$ at 200 °C. They concluded that circulation rates must be restricted to below 100 kg/s in a

reservoir volume of 0.125 km^3 and fraction spacing must be less than 100 m for reservoir lifetime to reach 30 years. Remoroza et al [2011] reached similar conclusions regarding drawdown based upon a 3D simulation. Brown [2000] assumes a 20 year reservoir lifetime and Dunn 2010 assumes 30 years. In this analysis, we assume 30-year lifetime for both the plant and the field.

4.3.2 Carbon capture

Ciferno [2006] reviewed amine-based CO_2 capture for retrofits to existing coal power plants. The CO_2 captured (CC) reduces plant CO_2 emissions but also decreases plant efficiency because heat is diverted from power generation to regeneration of the amine absorber. Hence, plant heat rate (HR), thermal energy required to produce a unit of electricity – BTU/kWh, increases with capture rate (CR - % CO2 captured). Table 1 displays heat rate adjustment factors (AF) relative to zero carbon capture based on Ciferno for several CR. They demonstrate substantial increases in heat rate associated with carbon capture. These factors also reflect parasitic losses to CO_2 compression, 0.12 KWh/kg-CO_2.

Fuel cycle emissions for power generation with carbon capture are modeled in this study from the emissions for a coal fired power plant in GREET1 [2012]. It is assumed that carbon capture will require sulfur removal upstream and that particulates will be removed in the overall process. Therefore, PM10, PM2.5, and SOx emissions are set to zero. Energy required for SOx and particulate control is negligible [Doctor 2011]. All other fuel-cycle emissions and energy consumptions at each CR are computed by multiplying the 0% carbon capture heat rate value (10,580 BTU/kWh) for a coal plant [GREET1 2012] by the heat rate adjustment factors (AF) given in Table 1. Total CO_2 generation, the sum of captured and emitted CO_2, at each CR is determined the same way. Those results are shown in columns 3 and 4 of Table 1.

Table 1: Summary of amine-based carbon capture in a coal power plant retrofit. The heat rate adjustment factor (AF) is from Ciferno [2006]. The last three columns are computed from the AF and GREET1 2012 as described in the text.

Capture rate CR	Adjust. Fctr. AF	Emitted CO_2 EC - g/kWh	Captured CO_2 CC - g/kWh	Effective heat rate[a] BTU/kWh
90%	1.434	152	1,364	9,842
70%	1.305	414	966	9,982
50%	1.197	632	632	10,123
30%	1.107	819	351	10,280
0%	1.000	1,057	0	10,580

[a] per combined coal and EGS power output - see below

The $scCO_2$ -EGS reservoir must be filled before operation, but the emissions for producing the initial $scCO_2$ charge are small relative to the emissions from producing and delivering the $scCO_2$. We estimate that the effect of neglecting the emissions from filling the reservoir is to underestimate GHG emissions by 1% for the 90% carbon capture efficiency case.

4.3.3 $scCO_2$ consumption

Brown [2000)] used experience from water-EGS field testing at Fenton Hill to predict 3 kg/s of $scCO_2$ consumption for a 10 MW power system (1,080 kg $scCO_2$ / MWh) while Pruess [2007] estimates consumption from 5% consumption of 22 kg/s $scCO_2$ flow per MW (3,960 kg $scCO_2$ /MWh). The average, 2,520 kg $scCO_2$ /MWh is used in this study.

As depicted in Figure 3, our systems is a coupled pair of plants, a coal and EGS facility where the former provides the latter with the scCO2 required for its operation. Hence, the total electricity produced for 1 MWh of EGS power is:

$$El_{tot} = Y/CC + 1 , \qquad (1)$$

where Y is the scCO2 consumption rate (g/kWh) of the EGS facility. Hence using the average consumption given above and the CC for 90%, El_{tot} is 2.85 MWh, 1.85 of which is from coal. At this capture rate, 65% of the power comes from coal. For the 30% capture rate, El_{tot} is 8.2 MWh. The effective heat rate of the combined system, column 5 of Table 1, is just the fossil heat rate of the CCS coal plant at each capture rate scaled by the corresponding ratio of coal to total system power, i.e. HR(CR) = 10,580 * AF(CR) * Y/CC / El_{tot}. The decrease in effective heat with CR seen in the table demonstrates that the power generated by the $scCO_2$ EGS plant using captured CO_2 more than offsets the energy consumed at the coal plant for carbon capture.

4.3.4 Pipeline requirements

Pipelines for $scCO_2$ delivery require materials for construction (plant cycle LCA) and require power for operation (fuel cycle LCA). Both of these depend upon the transportation distance. Two references [Dooley et al 2009, ICF 2009] discuss pipeline requirements in the US for carbon capture and sequestration (CCS). Dooley et al 2009 estimates tens of miles between source and sink. ICF 2009 considers $scCO_2$ pipeline infrastructure requirements that would be required to meet expected US CO_2 reduction mandates; therefore, the ICF analysis required estimation of pipeline distances to connect CO_2 sources to geological sequestration sites. They estimated an average distance of 50 miles per power plant if a common network infrastructure were built. Given the distance between power plants in the far west, where most geothermal power plants are located, is likely to be larger than this, we conservatively estimate a distance of 100 km (62 miles). It will be seen that this parameter has little effect on $scCO_2$ -EGS LCA.

Supercritical CO_2 pipelines require API 5L grade of X65 or X70 pipeline carbon steel for dry pumping, otherwise stainless steel when moisture is present. Economic flow velocities range between 1.5 to 2 m/sec [Element Energy Limited 2010]. Typical assumptions of pressures are approximately 15 MPa [ICF 2009].

Analysis of $scCO_2$ pipeline configurations (ICF 2009) demonstrated that the pipeline steel use (kg steel/m) per flow of $scCO_2$ (kg $scCO_2$ /s) is independent of pipeline diameter:

Pipeline steel use increases with pipeline diameter, but so too does the pipeline flow and the two effects cancel. Therefore, if steel is the overwhelming infrastructure material for the pipeline, then the pipeline configuration details will not affect the present analysis. The pipeline configurations in ICF International 2009 required 0.74 kg steel/m for each kg/s of $scCO_2$ flow when the $scCO_2$ velocity was 1.5 m/s. As an example, a 16" outside diameter trunk pipeline (0.42" wall thickness) uses 104 kg steel/m and, when operating with 1.5 m/s velocity flow across its 0.385 m inside diameter, transports 140 kg $scCO_2$ /s which would support 200 MW of $scCO_2$ power generation consuming 2,520 kg $scCO_2$ /MWh.

Gurgenci et al [2009] comment that pipeline, transmission lines, and power generation plant must be relocated every 15 years (presumably because of thermal draw-down). Assuming each deployment shifts the system 5 km, then the pipeline requirements will be the main trunk (100 km) amortized over the carbon flow accrued over the assumed 30-yr lifetime plus an additional 5 km of pipeline every 15 years. We neglect this additional 5 km.

4.3.5 Pipeline pumping

Pumping power is tabulated in ICF (2009) for several scenarios corresponding to several sequestered masses. If these powers support the average 50-mile transport distance studied in ICF 2009, then the average pumping power from that reference is 3.83×10^{-5} KWh/kg/km. The default value in GREET1 2012 is 3.18×10^{-5} KWh/kg/km. Using the default value, our assumed scCO2 consumption rate, and a 100 km pipeline, the pumping power is about 8 kWh per MWh generated. This is less than one percent of the output power.

4.3.6 $scCO_2$ infrastructure materials on site

Table 2a in Sullivan et al 2010 displays the material masses used to construct EGS wells and shows the materials for surface piping between well and plant. The surface piping is only 1.7%, 4.1%, and 1.7% of the cement, diesel, and steel for well construction. Therefore, differences in well spacing between $scCO_2$ and the EGS-50 case in Sullivan et al will have little effect on the materials analysis for $scCO_2$ compared to water-EGS. We make the approximation that the $scCO_2$ well casing diameters and properties are the same for $scCO_2$ -EGS wells and for water-EGS wells of equal depth. For these reasons, this analysis uses the infrastructure materials for the EGS-50 case in Sullivan et al 2010 for the $scCO_2$ case. Energy and emissions from infrastructure materials were extracted from GREET1_2012 for the EGS scenario with 6 km wells with 3 liners. The steel requirements were increased to account for the 100 km $scCO_2$ pipeline. The result is in Table 3. As in other analyses, we neglect infrastructure materials to connect the $scCO_2$ -EGS system to the grid even though it may be remote (Gurgenci 2009). While infrastructure related emissions determine the life cycle emissions for water-EGS, it will be seen below that $scCO_2$ -EGS emissions are dominated by the fuel cycle at the coal power plant. Therefore, further sensitivity analysis was not considered for the $scCO_2$ -EGS infrastructure.

Table 3: Plant cycle energy use and emissions for power plant infrastructure per unit of power at the plant gate computed by adding 100 km of $scCO_2$ pipeline to values for water-EGS in Sullivan 2010. Despite the 100 km length, the pipeline has a minor effect on power plant infrastructure related emissions and energy use.

	water-EGS	$scCO_2$ **-EGS**
Energy Use: BTU per MMBTU electricity		
Total energy	59,643	60,588
Fossil fuels	53,072	53,958
Coal	24,365	24,638
Natural gas	15,428	16,028
Petroleum	13,279	13,293
Total Emissions: grams per MMBTU		
VOC	0.830	0.837
CO	7.272	7.291
NOx	8.740	8.808
PM10	7.437	7.492
PM2.5	2.974	2.991
SOx	12.040	12.128
CH4	11.919	12.061
N2O	0.054	0.055
CO2	6,322	6,381
CO2 (w/ C in VOC & CO)	6,336	6,395
GHGs	6,651	6,713

4.4 Results

Figure 4 shows a set of fossil energy consumption curves relevant to the energy performance of our combined system. In the figure, total electricity is described by equation (1). The "coal standalone" (no carbon capture) and "CCS coal standalone" curves merely reflect their heat rates, the former without and the latter with a dependence on CR. In both of those cases, plant cycle energy is negligible. The most interesting dependence in the figure is shown by the "combined" curve, which shows a decrease in fossil energy consumption per unit power out. That energy is:

$$E_{fos} = [(HR(CR)/3413 * (1 + \varepsilon_e) + \mathcal{E}_{coal}) * Y/CC + \mathcal{E}_{egs}] / [Y/CC + 1], \qquad (2)$$

where ε_e (=0.02 for coal) denotes the ratio of upstream fuel production energy to the fuel use energy, and $\mathcal{E}_{coal}$ and $\mathcal{E}_{egs}$ denote the plant cycle energy ratios at the plant gate for coal and EGS plants. Values are the ratios are 0.0023 and 0.059, respectively. This curve, substantially the "CCS coal stand alone" curve adjusted by the ratio of coal to total system power, clearly demonstrates that the combined system uses less fossil energy for all CR per unit power output than the conventional coal plant. Also shown in the figure is the $scCO_2$ -EGS share of the total electricity produced by the combined system, i.e. the inverse of equation (1). Note that fossil fuel

used for the EGS plant cycle ($\mathcal{E}_{egs}$ = 0.059 MWh/MWh) contributes 2% or less of the total fossil energy use shown in Figure 4 for the combined plant, illustrating that infrastructure material related energy use is a minor effect for $scCO_2$ -EGS.

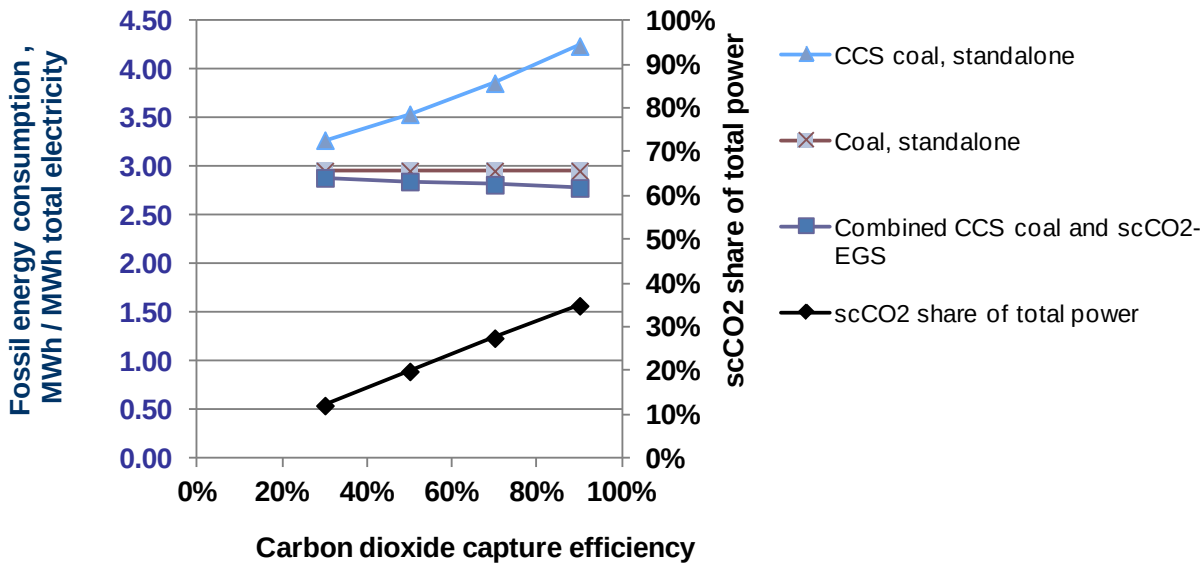

Figure 4: Fossil energy consumption and EGS share per total produced electricity at the plant gate.

Figure 5 shows four GHG emissions dependences on capture rate. The curve for the combination plant was determined from the following expression:

$$GHG(CR) = [\varepsilon_c * (EC + CC) + EC + ghg_{coal}]\ Y/CC + ghg_{egs}] \ / \ [Y/CC + 1], \qquad (3)$$

where ε_c is the ratio of upstream fuel production GHGs to those for fuel combustion (0.053 – from GREET1 2012), and "ghg" terms represent plant cycle emissions. GHG emission values (g/kWh) were obtained from GREET1 [2012] for both fuel and plant cycles and adjusted for CR as per equation (3). For CCS-coal stand alone case, equation (3) becomes:

$$GHG(CR) = \varepsilon_c * (EC + CC) + EC + ghg_{coal}, \qquad (4)$$

It is clear from the figure that GHG emissions per MWh decrease with carbon capture for a "CCS coal stand alone" plant but even more so for the combined system. This is, of course, due to the leveraging effect of EGS power. GHG emissions from the coal standalone plant are higher than either. The plant cycle ghg terms in equations (3) and (4) are 0.86 g/kWh for ghg_{coal} and 22.5 for ghg_{egs}, respectively. It is clear from the figure that ghg_{egs}, the largest of the two, makes a minor contribution to the total.

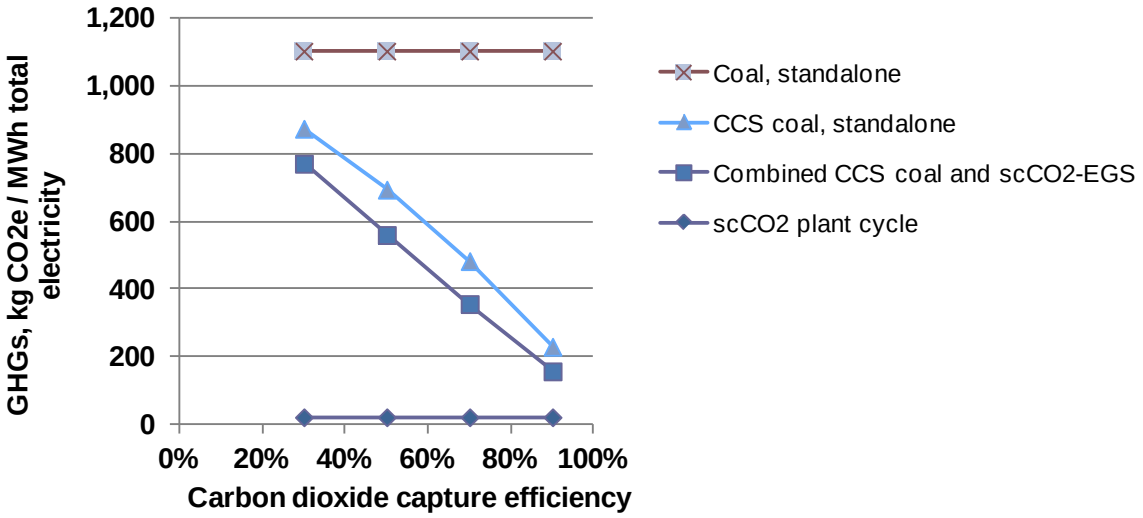

Figure 5: GHG emissions before transmission for $scCO_2$ -EGS power.

Figure 6 explores the effect of the $scCO_2$ consumption rate on changes in total greenhouse gases (ΔGHG) relative to conventional coal power at a series of capture rates (CR). This figure demonstrates that substantial reductions in GHG relative to those from a conventional coal plant can be achieved by coupling a CCS enable coal plant with a $scCO_2$ EGS facility. As expected, lower CR values results in lower GHG reductions.

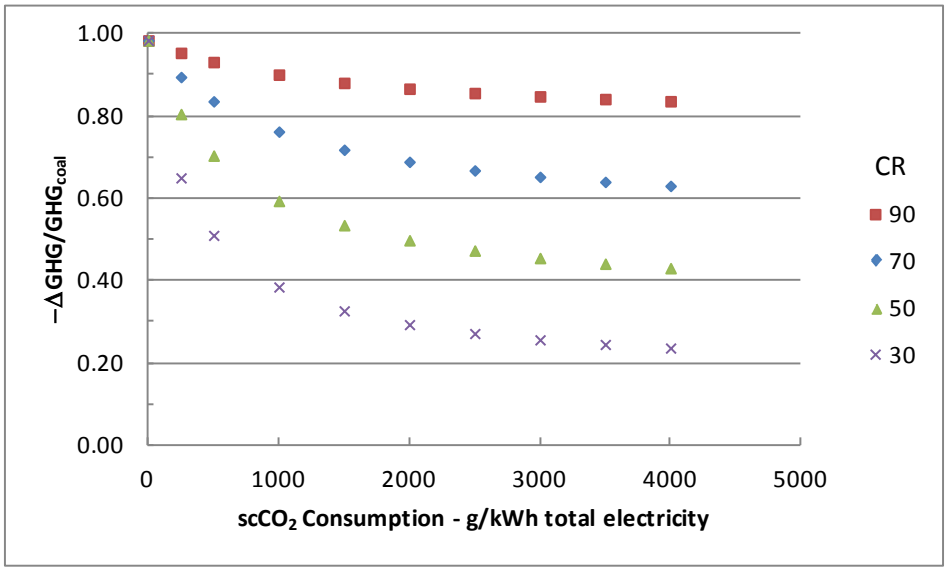

Figure 6: Reduction in GHGs vs. EGS $scCO_2$ consumption rates relative to GHG emissions from conventional coal for a combined CCS coal and EGS plant at several CO_2 capture rates.

Reading Figure 6 requires some care because the share of power from geothermal power varies across the abscissa. At low $scCO_2$ consumption, the geothermal plant provides most of the power because the geothermal plant is able to recirculate the $scCO_2$ many times before it is absorbed below ground. Thus, less $scCO_2$ is required from upstream and less coal-fired power is present in the mix. If the consumption rate is low enough that an on-site power plant can meet the demand, this may help deployment by eliminating the pipeline, but if $scCO_2$ -EGS is more useful by enabling CCS for the upstream power plant, then the low consumption rate reduces the ability to treat coal-fired GHG emissions.

Another factor considered for this analysis was leakage of reservoir CO_2 (kg/yr) to the atmosphere. Though there is considerable uncertainty on the magnitude of such a leakage due to the lack of field experience, we nonetheless made the following estimates. We assumed the leakage rate would be dependent on the amount of CO_2 in the ground; a first order dependence was considered a reasonable approximation. Further, it is important to account for the continual addition of $scCO_2$ to the reservoir during plant operation for every MWh produced. Hence, our governing rate equation becomes:

$$dM/_{dt} = -\alpha\, M(t) + R \qquad (4)$$

where M is the amount of CO_2 in the reservoir, α is the leakage rate (%/yr), and R is the rate of addition of CO_2 to the reservoir, in this case assumed to be 22.08×10^6 kg/yr (=2520 kg/MWh * 24*365) produced. Solving this equation for two regimes, one for the period during plant operation and the other for post decommissioning, we have:

$$M(t,\alpha) = M_o\, e^{-\alpha t} + R/_{\alpha}\, (1 - e^{-\alpha t}) \qquad (5)$$

for t ε (0, LT) and

$$M(t,\alpha) = M(LT)\, e^{-\alpha(t-LT)} \qquad (6)$$

for t ε (LT, t'). For these equations, M_o is the initial charge to the reservoir, assumed to be 5 million kg. Reservoir leakage emissions as a function of time are simply computed from $EM(t,\alpha) = M(t,0) - M(t,\alpha)$, where M(t,0) is simply the amount of material present in the reservoir at the starting time t for each regime, in this case 0 and LT for equations (5) and (6), respectively.

As already stated equation (4) is an approximation. Because our treatment of $scCO_2$ EGS power assumes a $scCO_2$ consumption rate, this admits to other loss mechanisms from the reservoir not accounted for, four of which were mentioned above. Hence, results based on equation (4) could be on the higher side.

Based on these expressions and assuming a 90% CR, we estimated the total cumulative CO_2 leaked from the reservoir after 100 years (30 years of operation and 70 years beyond decommissioning of both plants) to be 22 g/kWh, 208 g/kWh, and 1456 g/kWh, for α equal to

0.01%, 0.1%, and 1% per year, respectively. To these emissions we add 233 g/kWh of prompt emissions (life cycle GHG as per equation (3) and Table 1) from the coal plant to yield 159, 224, and 661 g/kWh, respectively, for the combined coal/EGS system (0.65 kWh from coal and 0.35 kWh from EGS). Despite greater overall fuel cycle GHGs generated by the combined plant [see Table 2; (CC+EC)*(1+ε_c)] at CR = 90% and taking into account reservoir leakage emissions, the above combined plant values are considerably less than prompt fuel cycle emissions of 1,102 g/kWh (equation 4 for CR=0) from a standalone coal plant.

Over a hundred years, much can happen to the CO_2 emitted to the atmosphere. In fact, there is a redistribution process for CO_2 emitted into the atmosphere. This process is known as the carbon cycle, which includes mechanisms whereby CO_2 emitted to the atmosphere is redistributed between the oceans, atmosphere and biosphere, resulting in a reduction of the added CO_2 in the atmosphere over time. A more complete discussion of this can be found elsewhere [Houghton, 1997]. Various models have been developed to quantify the fate of CO_2 emissions into the atmosphere; one such model is the Bern Carbon Cycle model [Joos et al, 2001]. A detailed discussion of that model is beyond the scope of the present study. Nonetheless, to account for the fate of CO_2 emitted into the atmosphere by our plant and reservoir, we employed a frequently used five term fit of the computed survival function [Shine et al, 2005; Hansen et al, 2007], i.e.

$$f(t) = a_o + \sum_1^4 a_i \, e^{-t/\tau_i} \qquad (7)$$

where a_i are dimensionless coefficients and τ_i are decay rates in years. The constants for this expression are: 0.18, 0.14, 0.18, 0.24, and 0.26 for the coefficients of $a_o \ldots a_4$, respectively, and 420, 70, 21, and 3.4 for the decay times of $\tau_1 \ldots \tau_4$, respectively [Shine et al 2005]. The sum of coefficients is unity. This expression represents model predictions for the fate of a pulse of CO_2 added to the atmosphere. The overall decay rate is very slow. In fact, after 100 years 33% of the original pulse still remains in the atmosphere; 22% remains after 500 years.

To calculate the reductions of the CO_2 added to the atmosphere, the following heredity integral is employed:

$$EM(t) = \int_0^t \dot{EM}(s) \; f(t-s) \, ds \qquad (8)$$

where EM is the remaining CO_2 emissions in the atmosphere, the dotted quantity is the time rate of CO_2 additions, and f(t) is the decay rate (survival function).

Employing equations (5)-(8), we calculated the time dependence of CO_2 emitted to the atmosphere. After 100 years, we find the remaining reservoir CO_2 emissions [EM(100)] to be 10, 99, and 662 g/kWh of EGS power for α of 0.01%, 0.1%, and 1% respectively. These values are 55% lower than their unadjusted counterparts given above. Clearly, this is a substantial reduction. Of the 233 grams of life cycle CO_2 per kWh emitted by the coal plant and its

associated upstream fuel production activities (given above), 82 g/kWh remain after 100 years. Combining this value with those remaining from EGS reservoir emissions, we estimate that total remaining CO_2 emissions are 56, 82, 290 g/kWh of combined EGS/coal power (same proportions as stated above) for α of 0.01%, 0.1% and 1%, respectively. Again, a 90% carbon capture rate was assumed. Further, even though atmospheric decay is delayed for reservoir CO_2 until it leaks out, the above values are still considerably less than 392 g/kWh remaining after 100 years from a standalone coal plant that had operated for the first 30 years.

4.5 Summary

The purpose of this study was to identify and explore the key parameters affecting the life cycle energy use and GHG emissions associated with producing geothermal electricity when $scCO_2$ is used as the thermal fluid. The technology is still theoretical and there is no demonstration yet. Therefore, we have used high-level parameters like CO_2 capture efficiency of coal power plants and $scCO_2$ consumption rate of geothermal facilities as the study parameters rather than mechanism level parameters like flow rates, mineralization rates, $scCO_2$ pressure and depth, etc., to describe the $scCO_2$-EGS system operating in steady state after the reservoir is fully charged. Had we attempted a mechanistic model, many parameters would have been introduced, like circulation rates and $scCO_2$ density, which would be speculative at this time, yet they have little *direct* bearing on an LCA analysis. Our approach expands the applicability of the study because by articulating the essential parameters from which life cycle results may be calculated, any particular mechanistic model, perhaps for a specific site, can estimate LCA results by computing the essential parameters described in our study

Our first result is that the few parameters introduced here, e.g., $scCO_2$ consumption expressed per unit of geothermal electrical energy produced, heat rate for the fossil power source generating the $scCO_2$, CO_2 capture efficiency, are adequate to support a high-level life-cycle analysis.

The second major result is that the $scCO_2$ geothermal power production must be considered in combination with the upstream $scCO_2$ production since both produce electricity and, thus, both contribute to the electrical-energy based functional unit. The energy consumption and emissions from electricity production associated with top-off $scCO_2$ production account for almost all of the emissions in the combined system. In particular, the emissions associated with plant infrastructure, including pipeline, are small in comparison. Even with 100 km of steel pipeline, the pipeline contributed only 1% of the plant-cycle GHG emissions in Table 3. The 100 km pipeline length assumption, then, had little effect on the analysis. Therefore, neglecting pipeline construction for periodic site relocation (Gurgenci 2009, mentioned in Section 3.2.1) will have minimal effect on LCA results.

As analyzed here, and for the assumed 2,520 kg $scCO_2$ /MWh, $scCO_2$ -EGS acts like an additional power cycle for the associated coal-fired plant. Renewable energy is being used to offset energy losses for CO_2 capture. Deployment will be limited by the number of situations in which a coal-power plant is located close enough to a geothermal resource. By contrast, water-EGS must have adequate water resources nearby and all of the water-EGS power is from renewable geothermal power.

5. Exploration

There are three important stages to developing and operating a geothermal power facility. They include field exploration, field development, and finally site operation. Ultimately, wells need to be drilled into a geothermal resource before a geofluid can be brought to the surface to produce power. However, drilling wells at a potential geothermal site is a very expensive undertaking and as such a geothermal developer must be convinced that a viable fluid resource is present before starting. In fact, it has been estimated that the exploration stage can comprise as much as 42% of overall project costs [Jennejohn, 2009]. Hence, exploration procedures have evolved to increase the success rate in developing geothermal resources. Such procedures can be divided into two critical groups: predrilling and drilling. In the predrilling stage, remote sensing, geochemical, and geophysical surveys are conducted on promising locations for assessing the presence and viability of potentially productive and cost effective geothermal resources. A detailed discussion of the specific methods employed in each of these surveys is beyond the scope of this study, but a good overview of them can be found elsewhere [USDOE, 2010].

Despite their cost impacts, predrilling methods have negligible impact on the total life cycle geothermal power as they are mostly analytical in nature. Nonetheless, a brief discussion of them is in order. Before land access rights are obtained, remote sensing technologies such as satellite, airborne hyperspectral, and light detection and ranging methods are employed to indicate the presence of a resource. If a promising resource appears to be present, land rights are obtained and a series of geochemical (CO_2 and Hg concentrations of fluids, elemental and isotopic ratios, temperature gradients, others) and geophysical (magnetotellurics, resistivity, gravity, seismic tomography, others) measurements are conducted. If the results from these surveys are sufficiently encouraging, a decision is made to drill exploratory wells.

Unfortunately, little to no published information is available on the number of exploration wells needed to confirm the viability of the geofluid resource. Average drilling success rates and associated ranges would be very useful for our life cycle assessments of geothermal power production. Sanyal and Morrow [2011] published a study on drilling success rates in the development and operational stages of existing geothermal fields, but unfortunately concluded that there is little information to establish success rates for the exploration stage. The two locations addressed in their study [Sanyal and Morrow 2011] were the Geysers and Kamojang steam fields.

In our earlier analysis of geothermal power production [Sullivan et al, 2010, 2011], we estimated the life cycle burdens of the exploration phase of well field development as one additional production well. Admittedly, this is an approximation, but a necessary one due to the dearth of information on how the exploration drilling phase of geothermal well field development is actually conducted. Further, this assumption implies that exploration wells have the same material requirements as production wells (and injection wells in the cases of EGS and HT-B plants). Generally, this is not the case. Exploration drilling is a combination of core holes, slim holes, thermal gradient holes, and finally confirmation wells. From a material demand point of view, only the last of these can be equated to a production well. Hence, exploration wells are typically lower in material and fuel demand than production and injection wells, but our having assumed their equivalence provided more conservative estimate of exploratory well burden, especially given the uncertainty about the number of such wells needed to confirm a site's resource potential. For the 10-MW HT-B system, the incremental cement, steel, and diesel fuel turned out to be about 22% of the existing burden for the production and injection wells. On the other hand, for the HT-Flash plant, the incremental burden was around 4.5%. The reason for the distinct difference between the two plants is related to plant capacity. As capacity increases, the greater is the number of wells required to support it, though the number of exploration wells in both cases was assumed to be one. The ratio of exploration to production/injection wells was 1:4.1 for the HT-B plant, whereas it was 1:20.6 for the HT-F plant.

To develop better estimates of the life cycle burdens for the exploration stage of geothermal power, we have developed the following alternative approach. It is an approach inferred from industry input to the GTP LCOE initiative. The scheme is:

1. Using a variety of geochemical and geophysical assessments, assess up to 5 sites with some potential.
    a. From these sites, identify 3 with the most potential
    b. Drill 5 to 7 core holes at each of these sites.
2. From this set of sites, choose 1 with the highest potential
3. At this site, drill a series of confirmation wells (assumed here to be production wells).
    a. Site is declared a success if 3 out of no more than 5 confirmation wells are productive. A probability of success is attached each confirmation well drilled.

For clarification purposes, we divide exploration into two stages: coring and confirmation.

We used this model to estimate life cycle burdens of exploration drilling for EGS, HT-B, and HT-F facilities. EGS and HT-B are typically hidden resources (not evident at the surface), whereas for HT-F there are usually surface manifestations (fumaroles, mud pots, geysers, others). We define a successful site after Sanyal and Morrow [2011] as one where geofluid flow rate and temperature from its wells are sufficient to meet cost effectively the desired plant power output. Drilling wells is a very expensive proposition and hence, companies developing GT sites must be reasonably certain that a profitably exploitable resource is present and accessible.

Toward that end, 5 to 7 core (slim) holes are drilled at the three sites. Boring these holes is much less expensive than drilling production wells. From those wells, the developer identifies two important findings: 1) the site with the most potential (highest resource temperature and potential flow rates), and 2) the subsurface distribution of the resource at the site. The latter informs the developer where best to drill confirmation wells at the site with the most potential. While thermal gradient holes are also used by field developers, they are not considered here because they are typically narrow holes often from drilled from the back of a truck and hence have negligible life cycle footprint.

Because there is no guarantee of success even after core hole surveying, a probability (P_1) is introduced to estimate the success rate for a confirmation well. Further, due to cost considerations, there is a limit on the amount of drilling that a developer is willing to do to ascertain a site's viability; in our treatment the maximum is assumed to be at most 5 confirmation wells.

Based on others [Jennejohn, 2009 and Benoit et al], we make the following core hole assumptions: 1) a 6¾ inch core hole is bored to a depth of ¼ of total well depth, which is subsequently cased with a 4½" casing and cemented in place, and 2) from there a 3.83 core hole bored rest of the way to targeted depth. For our analysis, cement and casing materials are assigned to the hole/well as they are permanently attached. Also attributed are the water and diesel fuel required to drill the well or hole from surface to the bottom. Core rods are not allocated to the well as they are assumed to be reusable. Confirmation wells are in practice production wells; the materials required for their construction have been discussed before [Sullivan et al, 2010, 2011]. As confirmation drilling in our model has a statistical component, the sum of average number of failed confirmation wells on a successful site plus average number of successful wells on failed sites plus or minus one standard deviation is attributed to the successful site. Successful confirmation wells on a successful site are considered production wells and hence attributed to well field development and not exploration.

The diesel fuel requirement is based on the daily fuel consumption rate for a 300 hp drilling rig (200 gallons/da) times the number of days required to drill the core holes. Based on Benoit et al, we assume that value to be around 34 days per km depth. Water consumption for core drilling is required in two places: 1) water for the cement in the cased zone of the core hole, and 2) mud needed for cooling the coring tool and for flushing cuttings away. Based on industry practice for drilling rotary cone bits, the mud and hence water requirements is typically around 5 times the volume of the well/bore hole. Due to the hollow structure of core bits, we assumed the mud requirements to be 5 times the volume of the hole minus the core.

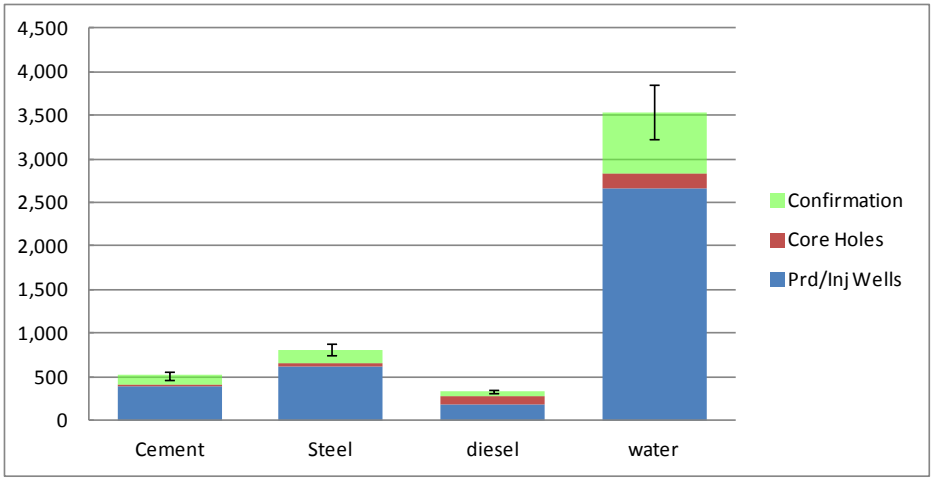

Figure 7: MPRs for a 20 MW EGS plant wells including 5 km production and injection wells, core and slim hole exploration, and confirmation wells; units are mt/MW for steel and cement, and kilo-liters/MW for water and diesel fuel; error bars are ±1 stdev for confirmation wells

It is expected that the well field exploration (coring and confirmation) process adds materials, water and diesel fuel to the overall life cycle for these facilities. The question is how much. Results from the model are shown in Figures 7 and 8. As seen in the figures exploration activities do contribute appreciably to well field MPRs. In fact for the EGS facility, the added steel and cement for exploration correspond to about 28% of their respective well field MPRs. Exploration diesel is about 45% of the diesel MPR. These percentages (not absolute amounts) are independent of well depth. On the other hand, exploration water consumption is only about 14% of total well field water consumption. This value is as low as it is due to well field stimulation, a process unique to EGS and typically requires large amounts of water. In this case, water for stimulation is about 7,800 kliters/MW, which is 50% of the well field water MPR.

The exploration percentages of well field MPRs increase with decreasing facility capacity. For example, the percentages of well exploration cement, steel, and water MPRs for a 10 MW HT-B plant range from 46% to 50%. Due to the absence of well field stimulation, the percentage of exploration water to its total well field MPR is sensibly the same as those for steel and cement. For diesel the percentage is about 68%. These values, all higher than those given above for the 20 MW EGS plant, are expected. As exploration is a onetime activity with a fixed burden employed to identify a geothermal resource, the greater is the output of the resource, which usually indicates more wells, the lower is the relative contribution of exploration to the overall life cycle burden of the facility. In fact, if we apply our exploration model to a 50 MW HT-F facility, exploration well field cement, steel and water amount to about 15% of their respective well field MPRs. However, the application of our model to HT-F facilities, which are generally sited where resources are conspicuous, might overestimate exploration life cycle burdens somewhat.

With the exception of diesel, three quarters or more of well field exploration cement, steel, and water burdens are attributable to confirmation well drilling. It is roughly opposite for diesel consumption, which is mostly employed during coring activities.

For the above set of estimates, we assumed that the success rate for confirmation wells drilling is 60%. If instead P_1 = 80% success rate is assumed, the exploration component of the MPRs are markedly reduced. For the 10 MW HT-B plant, exploration component of well field cement, steel, and water MPRs ranges from 25% to 30% and for diesel 60%, respectively, instead of the values given above. These values are markedly lower than the values cited above for this plant.

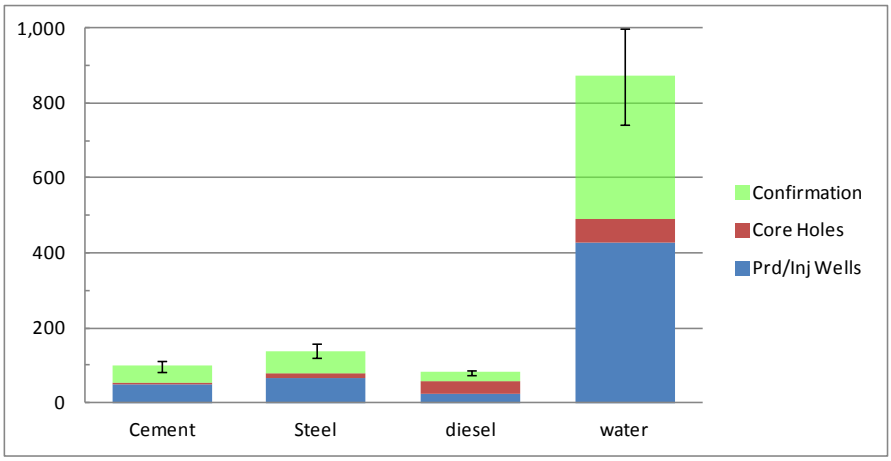

Figure 8: MPRs for a 10 MW HT-B plant wells including 1 km production and injection wells, core and slim hole exploration, and confirmation wells; units are mt/MW for steel and cement, and kilo-liters/MW for water and diesel fuel; errors bars are ± 1 stdev for confirmation wells.

The variations (range bars) shown in Figures 7 and 8 are derived solely from the confirmation well drilling stage. They are due to failed wells on successful sites plus successful wells on unsuccessful sites during confirmation drilling. For P_1 = 60%, they are roughly a third of the total exploration MPRs for water, cement, and steel, whereas it is about 15% for diesel fuel.

We have not conducted an estimate of exploration for GPGE operations. In the case of green field sites, it would be consistent with natural gas exploration of which we have no information. For reworked sites, the resource has already been developed albeit degraded by increased brine (geofluid) and reduced gas production. Hence for the latter, little if any additional exploration is expected.

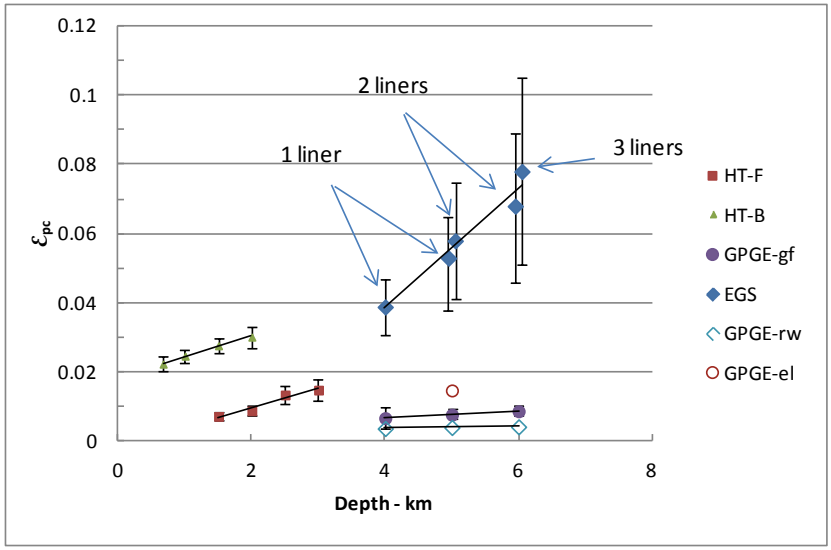

Figure 9: Plant cycle energy ratio for several geothermal energy technologies; range bars represent 1 standard deviation for EGS, HT-f, and HT-B; P_1=0.6

Figures 9 and 10 show $\mathcal{E}_{pc}$ and GHG_{pc} values for the geothermal power systems covered herein. These plant cycle values were computed using cement, steel, diesel, and other materials employed for exploration, confirmation, production, and injection well drilling, plant construction and materials, and above ground piping between wells and plants. As expected the figures show increasing values of $\mathcal{E}_{pc}$ and GHG_{pc} with well depth. Further, notice that $\mathcal{E}_{pc}$ and GHG_{pc} values for EGS systems are considerably larger than are those of the HT-F plants. There are two reasons for this result: (1) very large air-cooling structures required for binary plant condensers which comprises about half of the plant's steel and concrete; and (2) large amounts of cement, steel, and fuel are needed for drilling deep wells. Notice also that $\mathcal{E}_{pc}$ and GHG_{pc} for the HT-B plant are intermediate to those of EGS and HT-F technologies. This result is also expected. The HT-B system also uses air cooling systems, but at the same time, its wells are much shallower than those used in the EGS technology. Finally, HT-F has the lowest $\mathcal{E}_{pc}$ and GHG_{pc} values for power only geothermal technologies. These systems typically use water cooling, which are smaller structures than air coolers, and have comparatively high power output due to generally higher resource temperatures.

The range bars shown in Figures 9 and 10 arise from two effects: 1) variation in exploration drilling as discussed above, and 2) run to run differences in the number of wells required to meet design output power. The latter effect is a result of assumed variations in resource temperature, flow rates, the ratio of production to injection wells, and in the case of EGS the use of submersible pumps at the highest flow rates. From the lowest to highest well depths, the magnitudes of the ranges are: 24% to 38% for EGS, 16% to 21% for HT-F, and 7% to 10% for HT-B. Because the quantities plotted in Figures 9 and 10 are dependent on fixed and a well depth dependent variable term, the plots demonstrate a decreasing percentage of variation

with decreasing well depth. In short, as well depth decreases, topside plant structures and plant to well piping energy and emissions (the fixed term), increase their magnitude relative to the well (variable) term.

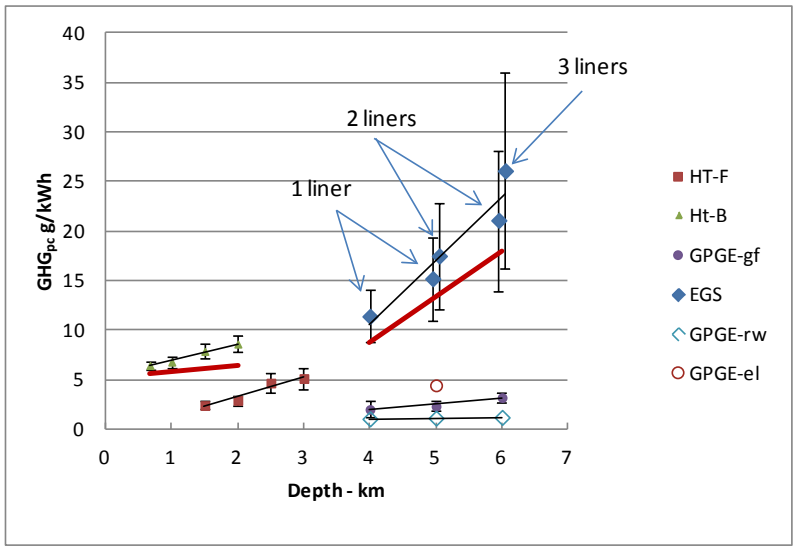

Figure 10: Plant cycle GHGs for several geothermal energy technologies; range bars represent 1 standard deviation for EGS, HT-f, and HT-B; solid red lines are for plants under the previous exploration scenario; P_1=0.6

The solid red lines seen in Figure 10 are trendlines from the previous [Sullivan et al, 2011] assessment of GHG_{pc} for our geothermal scenarios, where exploration was treated as one additional production well. Clearly, our current assessment shows a greater impact of exploration on GHG_{pc}. In fact, the differences between "old" and "new" trendlines range from 25% to 30% for EGS and 14% to 30% for HT-B. We don't show a previous trendline for HT-F as it is virtually on top of the current trendline. This is not unexpected. Because the HT-F facility has a 50 MW capacity and over 20 wells, its exploration stage as is treated herein is a comparatively small part of the overall GHG_{pc}.

Given the lack of useful information on geothermal well field exploration, our model was developed to fill that gap. While our scheme may not be representative of all exploration cases, it is an method based on a systematic approach used by one developer. Though perhaps some developers do not conduct all the drilling employed in our model, there is a good chance that they may use information based on drilling conducted by a different entity. And as far as our LCA is concerned, it is appropriate to include all data used to bring the power plant into operation, irrespective of when the data was gathered. It is widely viewed [Jennejohn, 2009; Fleischmann, 2006] that geothermal exploration drilling is a very expensive and risky undertaking and as such considerable preliminary drilling is necessary before committing to full scale development (drilling) of any potential well field.

6. GHG and Criteria Pollutant Emissions from Power Production

The generation of electricity in the United States is mostly derived from the combustion of fossil fuels. In the process of combustion, fossil fuels are consumed, fossil CO_2 is emitted, and other emissions like CH_4, N_2O, NO_x, SO_x, PM_{10}, $PM_{2.5}$, VOC, and CO are also emitted. The first two of these emissions are GHGs whereas the last six are criteria air pollutants henceforth denoted as (CAP). These are controlled emissions which are managed to meet air emission regulations by emission control and abatement systems added onto the power plants. The overall emissions generated during electricity production are substantial and driven by increasing demand for heat, light and power for machinery. And it could potentially grow considerably more when electrically powered vehicles begin to penetrate the vehicle marketplace. Almost 40% of U.S. primary energy is consumed by the electricity generating industry, about 70% of which is derived from fossil fuels (EIA, 2010).

The GREET model, developed by Argonne National Laboratory (GREET 1, 2012; Wang 1999), includes electricity generation for a wide range of generating technologies burning various fuels. The model includes the energy and emission factors for GHG and CAP for each technology and fuel combination. These emission factors, expressed as g/kWh, are important upstream parameters for estimating life-cycle emissions associated with consumption of electric power for stationary and transportation applications. In 2012, Argonne released an important update [Cai et al, 2012] on power plant emission factors, which have been integrate into the most recent version of GREET 1 [2012].

The study by Cai et al [2012] was a comprehensive effort that provided revised emission factors for a wide range of power generating technologies burning various fuels. While a detailed discussion of that work is beyond the scope of this study, a brief overview of their approach is merited.

Emission factors were developed for power derived from combustion of four main fuels: coal, natural gas, oil, and biofuels. Data were extracted from a number of sources including EPA's [2011] eGRID, EIA 923 [2007], and others. The focus of the update was primarily on emissions derived from power plant fuel consumption and not upstream emissions associated with fuel production or emissions associated with the plant cycle. While most plants burn only one fuel, a few burn more than one and they were taken into consideration on a fuel/power technology basis. Some plants provided a combination of heat and power. They were not included due to issues around allocation of burdens to each energy output, i.e. heat and power. Plant energy conversion efficiencies (on a low heat value basis), technology distributions, and fuel composition (e.g. carbon and sulphur content) were considered from which emissions factors were developed on both a national and state by state basis.

A statistical analysis was also conducted. On the basis of the updated GHG and CAP emission factors and energy efficiencies for the various power technologies by fuel type, the

probability distribution functions were developed to describe the relative likelihood for the emission factors and energy efficiencies as a function fuel type and generating technology. This was done on a national average basis.

Also recently added to GREET1 [2012] were plant cycle energy and GHG and CAP emissions for the various power generating technologies, fossil and renewable. Included in this addition were energy and emissions for three geothermal technologies, namely EGS, HT-B, and HT-F. Plant cycle additions to GREET were based on the LCAs conducted previously [Sullivan et al, 2010, 2012] for the geothermal effort.

Figure 11 (values in Table A-2) summarizes, by life-cycle stage, our life-cycle GHG emissions estimates (in g/kWh) for the various power technologies considered herein. The values shown in the figure are averages. The figure is consistent with our previous conclusions (Sullivan et al., 2010). The strictly fossil fuel plants generate much more GHGs per kWh than their renewable, hybrid, and nuclear counterparts. As expected, IGCC power has lower GHG emissions than its conventional thermoelectric counterparts for coal and biomass. This is a consequence of the greater efficiency of IGCC technologies. For the fossil electricity plants, the preponderance of GHG arises from the fuel burned to produce the electricity.

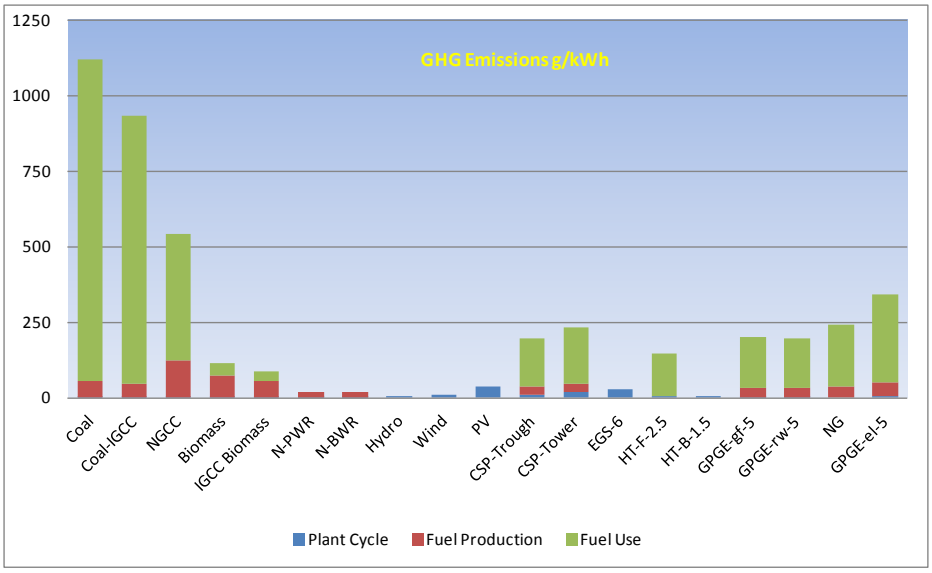

Figure 11: Greenhouse gas emissions (g/kWh) by life-cycle stage for various power production technologies relative to total energy output (electricity and/or NG); entries are based on average MPRs given above and GREET1_2012 data; numerical postscripts denote well depths in km.

All plants shown in Figure 11 have GHG emissions in one or more of the stages in their life cycles. For example, all plants have emissions in their plant cycle stage, though not conspicuous in the figure for many of them. Further, GHGs are emitted during the fuel production stage for fossil, biomass, nuclear, and the hybrid technologies, and during the fuel use

stage for fossil, hybrids, biomass, and HT-F. The percentage of renewable energy output for the hybrid technologies was assumed to be 85% for CSP, 17% for GPGE-rw and GPGE-gf, and 31% for GPGE-el; the balance in each case was fossil based electricity.

Of the renewable technologies, hydro, wind, PV, EGS and HT-Binary have the lowest GHG emissions, whereas HT-Flash and biomass power have the highest. In either case, they are considerably lower than those from the strictly fossil fueled power plants. For HT-Flash, the GHGs are, as discussed above, fuel-use emissions, which come primarily from dissolved CO_2 in the geofluid that is released to the atmosphere upon its passage through the plant. GHGs are emitted during biomass production and use, and arise from fuel use in harvesting forestry residues and incomplete combustion yielding methane nitrous oxide (N_2O) emissions during fuel use. The hybrid plants (GPGE and CSP) have higher GHG emission rates than those from the renewable technologies, though still considerably lower than those from strictly fossil fueled plants. This is a consequence of their dual output, one fossil (natural gas) and the other renewable (geofluid power). Due to comparatively minor material and fuel requirements for reworking a GPGE site or drilling a new green field site, their GHG values are sensibly the same.

For comparison purposes, a natural gas (NG) production and use bar (from GREET1_2012) has been added to Figure 11, representing the production of solely natural gas from associated wells and its combustion in a utility/industrial boiler. When this bar is compared to those for the GPGE-gf and GPGE-rw dual-output systems (gas and electricity), it is seen to be conspicuously higher because its lacks the leveraging effect of the dual output GPGE plants. The electric-power component of the GPGE dual output emissions arise from the plant cycle stage and is very small (barely visible in the figure).

Despite its consumption of about twice the natural gas as simply producing and delivering a unit of natural gas to a consumer, the GHG emissions from the GPGE-el plant are only somewhat higher than those for natural gas production and delivery. This is due to geofluid powered electricity production, which is about a third of the systems output. For the same reason, its GHG emissions are lower than those of a comparable NGCC plant.

Criteria pollutant emission (CAP) results generated from GREET1 [2012] for the various power generation technologies are shown in Figure 12. Because of the range of emission levels, the results are presented on a logarithmic scale. Though GREET1 reports both 2.5- and 10-micron PM, to reduce clutter the plot shows only PM10 results. Data values are given in Table A-1 in the appendix. From an inspection of the figure, it is clear that the strictly combustion-based electric power-generating technologies, shown at the graph's left side, including biomass fueled technologies, overall generate one or more orders of magnitude more CAP emissions than those of nuclear and the renewable technologies. The emissions from the GPGE facilities (on the right side of the figure) are only marginally lower than those from the strictly combustion based plants. Although the dominant energy output from the GPGE dual output facilities is natural gas, its associated emissions relative to those for strictly natural gas production are weighted

downward somewhat by its geothermal electricity output. On the other hand, when a GPGE-el facility is compared to NGCC, its strictly fossil counterparts, its emission performance is somewhat better, again due to the leveraging effect of geothermal power output. However, overall, emissions from GPGE-rw, GPGE-gf, NG, and GPGE-el are quite similar.

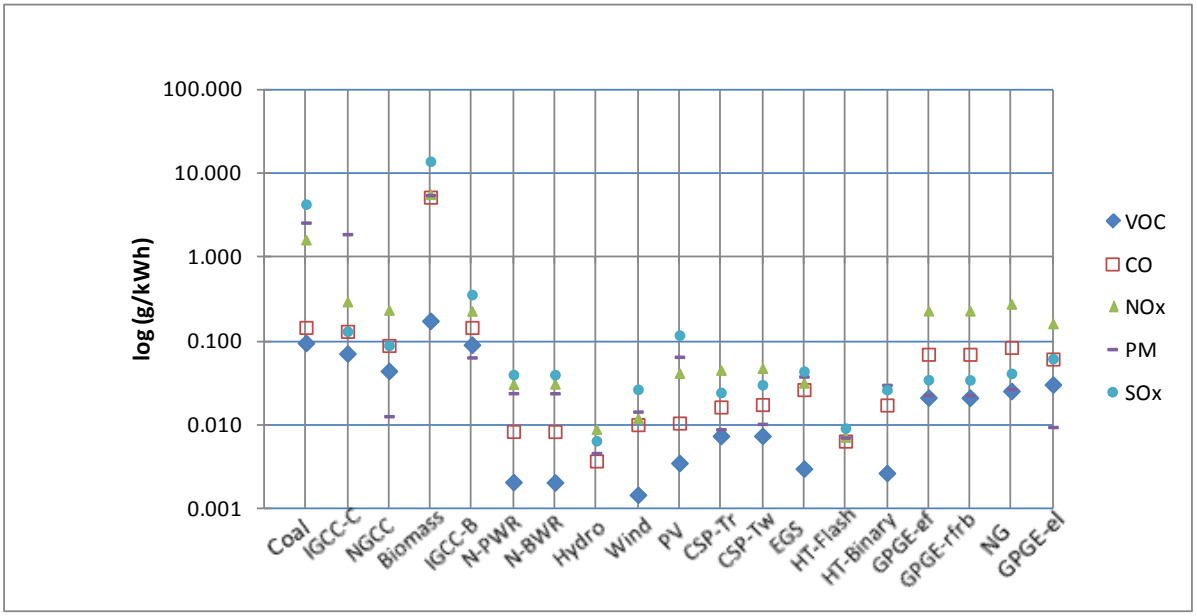

Figure 12: Criteria pollutant emissions (g/kWh) over the life cycles of various power-production technologies.

With the exception coal and biomass boiler power, on balance SOx emissions for the rest of the technologies are roughly 0.032 g/kWh. The comparatively high SOx values for coal is related to sulphur contents of the fuels. As for biomass, the high concentration of sulphur emissions is a result of cofueling those plants with a high percentage of municipal solid waste and black liquor from the paper industry. Notice that their IGCC counterparts have much lower SOx emissions. This is a consequence of IGCC technology where sulphur gases must be scrubbed from the synthesis gas before combustion. With the exception of SOx emissions, PV life cycle CAPs are in good accord with those of the other renewable technologies. Its somewhat higher SOx value is a consequence of plant cycle emissions associated with copper and silicon production.

VOCs are consistently below 0.01 g/kWh and NOx emissions below 0.1 g/kWh for the renewable and CSP technologies, though the latter a hybrid technology tends to be on the higher side of that grouping. On the other hand, VOC and NOx emissions are considerably higher (sometimes by more than an order of magnitude) than combustion based technologies, which includes the GPGE scenarios for either dual gas and electric or all electric outputs. The CO emissions for the renewable and CSP technologies as a group range around 0.013 g/kWh, and as such are conspicuously lower than those for the combustion based technologies, albeit a little

less so for the GPGE set. While CSP technologies have been assumed to be hybrid technologies, their fossil profile is considerably lower when compared to GPGE and consequently their CAP emissions more closely resemble those of the renewable technologies. And finally, with the exception of coal boiler, IGCC coal, and biomass boiler technologies, particulate emissions (PMs) appear to range widely between 0.005 and 0.0065 g/kWh.

Overall, the GHG and CAP emissions are as expected: higher for combustion based power, intermediate for hybrid power, and lowest for renewable power. In the case of renewable technologies, their GHG and CAP emissions arise from the plant cycle only, a one time charge of emissions (except for HT-F GHGs) over plant lifetime. Results clearly show that GHG and CAP emissions from geothermal facilities are very much less than those from the strictly fossil based technologies, lower than those from the hybrid technologies, and mixed for those of the renewable technologies. Among the geothermal technologies, HT-B has the lowest GHGs which are on a paar with hydro and wind; EGS has midrange GHGs which are on a par with PV, and HT-F has the highest, which are incurred during plant operation.

7 Conclusions

A number of important issues with geothermal power have been addressed. These topics included GHG emissions from hydrothermal flash plants, use of supercritical CO2 as a working fluid for EGS, a model for estimating the impact of geothermal field exploration on geothermal life cycles, and finally an analysis of GHGs and CAP from a variety of power plants including geothermal plants.

An analysis of California GHG emissions from geothermal plants was conducted using DOE power generation data to develop an emissions distribution function from flash and dry stream geothermal plants in California. From that analysis, it is found that the GHG emissions range from 11 to 370 g/kWh with a weighted average of 98 g/kWh. Our view is that these results are a good preliminary estimate of California geothermal GHG emissions. Limitations of the data were discussed as well as when new and better data maybe released.

A model was developed to estimate the life cycle burdens of geothermal systems (EGS) utilizing $scCO_2$ as a working fluid. The model represents a coupled system comprised of coal and EGS plants where captured CO_2 from former is compressed and pumped via pipeline to latter to serve as makeup $scCO_2$ offsetting reservoir losses. These losses are considered to provide a sequestration mechanism for the coal plant. Upon adjusting power output from coal plant for carbon capture and combining with EGS power output, enabled by the $scCO_2$, net energy and emissions associated with the coupled system were computed. Relative to a standalone CCS coal plants, to combined plant demonstrated substantial reductions in fossil energy consumption and atmospheric CO_2 emissions. The magnitude of these savings were found dependant on the $scCO_2$ consumption rate and carbon capture efficiencies, the latter of which ranged from 0% to 90%.

Also accounted for where reservoir leakage rates and concomitant atmospheric reductions of both prompt and leaked CO_2 due to repartitioning of the gas between the atmosphere, oceans, and biosphere.

The potential for sequestering a substantial fraction of coal power generated CO_2 emissions with $scCO_2$ -EGS in the US is likely limited because of the distributed nature of the existing coal plant infrastructure and the need for proximity to a geothermal resource. Nevertheless, $scCO_2$ -EGS consumption of coal power CO_2 could provide an energy and emission value when fossil fuel power plants and geothermal resources coincide, cost permitting.

To compensate for a lack of quantitative information on the magnitude of exploration well field drilling, a model was developed to improve our previous estimate for this stage's life cycle burdens, i.e. one additional production well. The model is based on some industry input about the extent of exploration drilling. It follows a scheme of drilling core holes on several sites, one of which is chose for confirmation well drilling. A probability of success is attached for each confirmation well drilled. Our new exploration estimates indicate a 25 to 30% increase in plant cycle GHG emissions for EGS, 14 to 30% for HT-B, and little change for HT-F over previous values. Exploration results are dependent on well depth.

Finally, an analysis was conducted on the overall GHG and CAP emission from a wide range of power generation technologies including fossil, renewable, and hybrid. As expected, the renewable and hybrid technologies have far fewer GHG and CAP emissions than the strictly fossil plants. Renewable plants in general have the least. GHG and CAP emissions from geothermal facilities are small and arise primarily from the plant cycle, though flash plants have some GHG emissions during the operational stage. However, they are still less than those from hybrid plants.

Acknowledgements
The Geothermal Technologies Program in the U.S. Department of Energy's Office of Energy Efficiency and Renewable Energy sponsored this work. Argonne National Laboratory is a DOE laboratory managed by UChicago Argonne, LLC, under Contract No. DE-AC02-06CH11357. We are grateful to Arlene Anderson of the Geothermal Technologies Program for her guidance and input.

Appendix A:

Table A-1: CAP Emissions for various power generation technologies: all units are g/kWh$_{elec.}$

Emission	Coal	Coal IGCC	NGCC	Biomass	Bio-IGCC	Nuc-PWR	Nuc-BWR	Hydro	Wind	PV
VOC	0.095	0.071	0.044	0.174	0.090	0.002	0.002	0.000	0.001	0.004
CO	0.146	0.131	0.089	5.200	0.145	0.008	0.008	0.004	0.010	0.011
NOx	1.617	0.295	0.235	5.631	0.229	0.031	0.031	0.009	0.012	0.042
PM10	2.000	1.502	0.008	3.103	0.040	0.018	0.018	0.003	0.011	0.049
PM2.5	0.585	0.381	0.005	2.400	0.024	0.006	0.006	0.001	0.004	0.016
SOx	4.291	0.131	0.089	13.908	0.359	0.040	0.040	0.006	0.027	0.118
CH4	1.583	1.302	3.505	0.689	0.088	0.044	0.044	0.004	0.026	0.063
N2O	0.0179	0.0407	0.0015	0.0812	0.1010	0.0002	0.0002	0.0000	0.0001	0.0005

Table A-1: (cont) CAP emissions from various power generating technologies: all units are g/kWh$_{all_outputs}$

Emission	CSP –tr	CSP-tw	EGS	HT-F	HT-B	GPGE-gf -	GPGR-rw	NG	GPGE-el
VOC	0.007	0.007	0.003	0.001	0.003	0.021	0.021	0.025	0.030
CO	0.016	0.018	0.026	0.006	0.017	0.070	0.070	0.084	0.061
NOx	0.045	0.048	0.032	0.007	0.028	0.230	0.230	0.277	0.162
PM10	0.006	0.008	0.027	0.005	0.020	0.012	0.012	0.014	0.006
PM2.5	0.003	0.003	0.011	0.002	0.010	0.011	0.011	0.013	0.004
SOx	0.024	0.030	0.044	0.009	0.026	0.035	0.034	0.041	0.062
CH4	0.541	0.544	0.043	0.760	0.040	1.539	1.539	1.859	2.412
N2O	0.0003	0.0003	0.0002	0.0000	0.0002	0.0034	0.0034	0.0041	0.0011

References

Benoit, D., Moore, J. and Goranson, C., Core Hole Testing and Drilling at the Lake City, California Geothermal Field, https://pangea.stanford.edu/groups/.../**Core**%20**Hole**%20**Drilling**.pdf, accessed 4/30/2012

Bertani, R., and Thain, I., 2001, *Geothermal Power Generating Plant CO_2 Emission Survey*, Rev. 1.0, International Geothermal Association, http://www.jeotermaldernegi.org.tr/ian%20i.htm, accessed August 2010.

Bloomfield, K.K., Moore, J.N., and Neilson, Jr., R.M., 2003, Geothermal Energy Reduces Greenhouse Gases, *Climate Change Research*, March/April, 77–79.

Brown D W 2000 A hot dry rock geothermal energy concept utilizing supercritical CO2 instead of water *Proceedings, Twenty-fifth workshop on geothermal reservoir engineering, Stanford, California, January 24-26 2000 SGP-TR-165* (Stanford, CA: Stanford University)

Cai, H., Wang, M.Q., Elgowainy, A., and Han, J., 2012, Updated Greenhouse gas and Criteria Air Pollutant Emission Factors and Their Probability Distribution Functions for Electric Generating Units, ANL/ESD/12-2.

Ciferno J 2006 CO_2 Capture from Existing Coal-Fired Power Plants (available at http://www.netl.doe.gov/energy-analyses/pubs/CO2%20Retrofit%20From%20Existing%20Plants%20Revised%20November%202007.pdf, accessed 3 February 2012)

Clark, C.E., Harto, C.B., Sullivan, J.L., and Wang, M.Q., 2011a, *Water Use in the Development and Operation of Geothermal Power Plants*, ANL/EVS/R-10/5.

Clark, C.E., Harto, C.B. and Troppe, W.A., 2011, Water Resource Assessment of Geothermal Resources and Water Use in Geopressured Resources, ANL/EVS/R-11/10.

CEPA, 2010, Air Resources Board, Reported Emissions, Facility Emissions, http://www.arb.ca.gov/cc/reporting/ghg-rep/ghg-rep.htm, accessed August 16, 2011.

Doctor R 2011 Economic comparison of CO_2 capture and sequestration from amines and oxyfuels. Report to Environmental Projects Division, U.S. Department of Energy, National Energy Technology Laboratory. December 29 2011. Morgantown

Dunn P 2010 Baseline System Costs for 50.0 MW Enhanced Geothermal System. *GSPAWG Meeting, November 17-18 2010* (Washington, D.C.: Department of Energy)

EIA (Energy Information Administration), 2010, *Annual Energy Outlook 2010*, Tables 85 and 101 [http://www.eia.doe.gov/oiaf/aeo/], accessed August 2010.

EIA-923, 2010, Department of Energy, The Energy Information Administration (EIA), 2010, EIA-923 Monthly Time Series File, Sources EIA-923 and EIA-860, http://www.eia.gov/electricity/data/eia923/, Accessed 6/25/2012.

EPA, 2011a. The Emissions & Generation Resource Integrated Database (eGRID 2010 Version 1.1), http://www.epa.gov/cleanenergy/energy-resources/egrid. Accessed March 2012.

Fleischmann, D. J., 2006, Geothermal Resource Development Needs in Arizona, Geothermal Energy Association, GEA, http://geo-energy.org/plants.aspx, Accessed 4/15/2012.

Frank, E. D., Sullivan, J. L. and Wang, M.Q., 2012, Life cycle analysis of geothermal power generation with supercritical carbon dioxide, Environ., Res. Lett., 7, open access

GREET1, 2012, Greenhouse Gases, Regulated Emissions and Energy in Transportation (GREET) model, http://greet.es.anl.gov/greet_1_series, last accessed 7/31/2012.

Houghton, J. T., 1997, Global Warming, Cambridge University Press, Cambridge, UK.

Jennejohn, D., 2009, *Research and Development in Geothermal Exploration and Drilling*, Geothermal Energy Association, Washington, D.C.

Joos, F., ,Prentice, I. C., Sitch, S, Meyer, R., , Hooss, G., Plattner, G.K., Gerber, S., and Hasselman, K., 2001, Global warming feedbacks on terrestrial carbon uptake under Intergovernmental Panel on Climate Change (IPCC) emission scenarios, GLOBAL BIOGEOCHEMICAL CYCLES, VOL. 15(4), 891-907.

Hansen, J., Sate, M., Kharecha, P., Russell, G., Lea, D. W. and Siddall., M., 2007, Climate change and trace gases, Phil. Trans. R. Soc., A, 365: 1925-1954.

Mobley R 2011 Baseline System Costs for 50.0 MW Enhanced Geothermal System. GSPAWG Meeting, August 24 2011. Washington, D.C.

Nelson C R, Evans J M, Sorensen J A, Steadman E N and Harju J A 2005 *Factors affecting the potential for CO2 leakage from geological sinks* (Grand Forks, ND: University of North Dakota) (available at http://www.undeerc.org/PCOR/newsandpubs/pdf/FactorsAffectingPotential.pdf)

Pruess K and Azaroual M 2006 On the feasibility of using supercritical CO2 as heat transmission fluid in an engineered hot dry rock geothermal system *Proceedings, Thirty-first workshop on geothermal reservoir engineering, Stanford University, Stanford, California, January 30-February 1, 2006 SGP-TR-179* (Stanford, CA: Stanford University)

Pruess K 2007 Enhanced Geothermal Systems (EGS): Comparing Water and CO2 as Heat Transmission fluids *Proceedings, New Zealand Geothermal Workshop 2007, Auckland, New Zealand, November 19-21,2007 LBNL-63627* (Berkeley, CA: Lawrence Berkeley National Laboratory) (available at http://www.osti.gov/bridge/product.biblio.jsp?query_id=5&page=0&osti_id=922829)

Remoroza A I, Moghtaderi B and Doroodchi E 2011 Coupled Wellbore and 3D Reservoir Simulation of a CO2 EGS *Proceedings, Thirty-Sixth Workshop on Geothermal Reservoir Engineering Stanford University, Stanford, California, January 31 - February 2, 2011 SGP-TR-191* (Stanford, CA: Stanford University)

Sanyal, S. K. and Morrow, J. W., 2011, An Investigation of Drilling Success in Geothermal Exploration, Development and Operation, GRC *Transactions*, Vol. 35, 233-237.

Shine, K. P., Fuglestvedt, J. S., Hailemariam, K., and Stuber, N., 2005, Alternatives to the global warming potential for comparing climate impacts of emissions of greenhouse gases, Climate Change, 68: 281-302.

Sullivan, J. L., Clark, C. E., Han, J., and Wang, M., 2010, *Life Cycle Analysis Results of Geothermal Systems in Comparison to Other Power Systems*, ANL/ESD 10-5.

Sullivan, J. L., Clark, C. E., Yuan, L., Han, J., and Wang, M., 2011, *Life Cycle Analysis Results of Geothermal Systems in Comparison to Other Power Systems*, Part II, ANL/ESD 11-12.

Tester J. W., Anderson B., Batchelor A., et al 2006 The future of geothermal energy: impact of Enhanced Geothermal Systems (EGS) on the United States in the 21st Century. Final Report to the US Department of Energy Geothermal Technologies Program (Cambridge, MA: Massachusetts Institute of Technology)

USDOE, 2010, *A History of Geothermal Energy Research and Development in the United States, 1976–2006, Volume 3: Reservoir Engineering*, http://www1.eere.energy.gov/geothermal/pdfs/geothermal_history_3_engineering.pdf, accessed March 16, 2011.

Wang, M., 1999. GREET 1.5—Transportation Fuel-Cycle Model, Vol. 1: Methodology, Use, and Results, Report No. ANL/ESD-39, Argonne National Laboratory.

Energy Systems Division
Argonne National Laboratory
9700 South Cass Avenue, Bldg. 362
Argonne, IL 60439

www.anl.gov

Argonne National Laboratory is a U.S. Department of Energy
laboratory managed by UChicago Argonne, LLC